Applied Catalysis B: Environmental 191 (2016) 29–41

Contents lists available at ScienceDirect

Applied Catalysis B: Environmental

journal homepage: www.elsevier.com/locate/apcatb

Carbon nanotubes containing oxygenated decorating defects as metal-free catalyst for selective oxidation of H_2S

Cuong Duong-Viet[a,b,**], Yuefeng Liu[a], Housseinou Ba[a], Lai Truong-Phuoc[a], Walid Baaziz[a], Lam Nguyen-Dinh[c], Jean-Mario Nhut[a], Cuong Pham-Huu[a,*]

[a] Institut de Chimie et Procédés pour l'Energie, l'Environnement et la Santé (ICPEES), ECPM, UMR 7515 du CNRS-Université de Strasbourg, 25 Rue Becquerel, 67087 Strasbourg Cedex 02, France
[b] Ha Noi University of Mining and Geology, 18 Pho Vien, Duc Thang – Bac Tu Liem – Ha Noi, Viet Nam
[c] The University of Da-Nang, University of Science and Technology, 54 Nguyen Luong Bang, Da-Nang, Viet Nam

ARTICLE INFO

Article history:
Received 20 November 2015
Received in revised form 20 February 2016
Accepted 9 March 2016
Available online 10 March 2016

Keywords:
CNTs oxidized
Acid treatment
HNO_3
N-CNTs
Selective oxidation of H2S

ABSTRACT

In this study, we report on the influence of gaseous HNO_3 treatment, with various time and temperature, on the creation of defects decorated with oxygenated functional groups on the CNTs side-wall. The gaseous acid treatment leads to a significant increase of the oxygenated functional groups and defects on the tube wall along with a specific surface area improvement. The as-synthesized catalyst was further used as a metal-free catalyst in the selective oxidation of H_2S in the waste effluents. According to the results the defects decorated with oxygenated groups are extremely active for performing partial oxidation of H_2S into elemental sulfur. The desulfurization activity is extremely high and stable as a function of time on stream which indicates the high efficiency of these oxidized un-doped carbon nanotubes as metal-free for the selective oxidation process. The high catalytic performance was attributed to both the presence of structural defects on the carbon nanotubes wall which acting as a dissociative adsorption center for the oxygen and the oxygenated functional groups which could play the role of active sites.

1. Introduction

Since the last decades, carbon nanomaterials, i.e., nanotubes (CNTs) and nanofibers (CNFs), have received an ever increasing scientific interest for being used as catalyst support or directly as metal-free catalysts in numerous relevant catalytic processes [1–6]. When used as catalyst support the defects and oxygenated functional groups present on the surface of these carbon nanomaterials play a key role to anchor metal and/or oxides nanoparticles active phase, which contribute to prevent excessive sintering of the metal and/or oxide nanoparticles during the course of the reaction [7–9]. The defects and oxygenated functional groups density on the CNTs surface can be enhanced by submitting the materials to oxidative process either in the presence of oxygen containing gas or in the presence of difference oxidation agents such as H_2O_2 [10], O_3 [11], $KMnO_4$ [12], $(NH_4)_2S_2O_8$ [13] and H_2SO_4 and/or HNO_3 [14–18]. Among these oxidation processes the gas-phase treatment seems to be the most efficient and appropriate to introduce defects and oxygenated functional groups without destroying the size and shape of the carbon nanomaterials [19,20]. However, these oxygen/defects functionalized carbon nanomaterials have mostly employed as catalyst support while they have rarely been tested directly as metal-free catalyst where defect sites and/or oxygen functionalities could play a pivotal role to activate the reactant.

Recently, nitrogen-doped CNTs composite has been reported to be an efficient metal-free catalyst for several relevant catalytic processes. In some catalytic processes the doped carbon nanomaterials exhibit even a better catalytic performance compared to traditional catalysts such as selective dehydrogenation of ethylbenzene to styrene, either in the direct or oxidative dehydrogenation processes [21], selective oxidation [22–27], oxygen reduction reaction (ORR) [28–30] or in other catalytic processes [31,32], just to cite a few. The catalytic activity was attributed to the dissociative adsorption of the oxygen molecule on the carbon localized close to the nitrogen site with electron deficient character according to the pioneering work of Dai and co-workers [33]. In the partial oxidation of H_2S into elemental sulfur such N-CNTs also exhibit an extremely high stability as a function of time on stream even under

* Corresponding author.
** Corresponding author at: Institut de Chimie et Procédés pour l'Energie, l'Environnement et la Santé (ICPEES), ECPM, UMR 7515 du CNRS-Université de Strasbourg, 25 rue Becquerel, 67087 Strasbourg Cedex 02, France.
E-mail addresses: duongvietcuong@humg.edu.vn (C. Duong-Viet), cuong.pham-huu@unistra.fr (C. Pham-Huu).

http://dx.doi.org/10.1016/j.apcatb.2016.03.018
0926-3373/

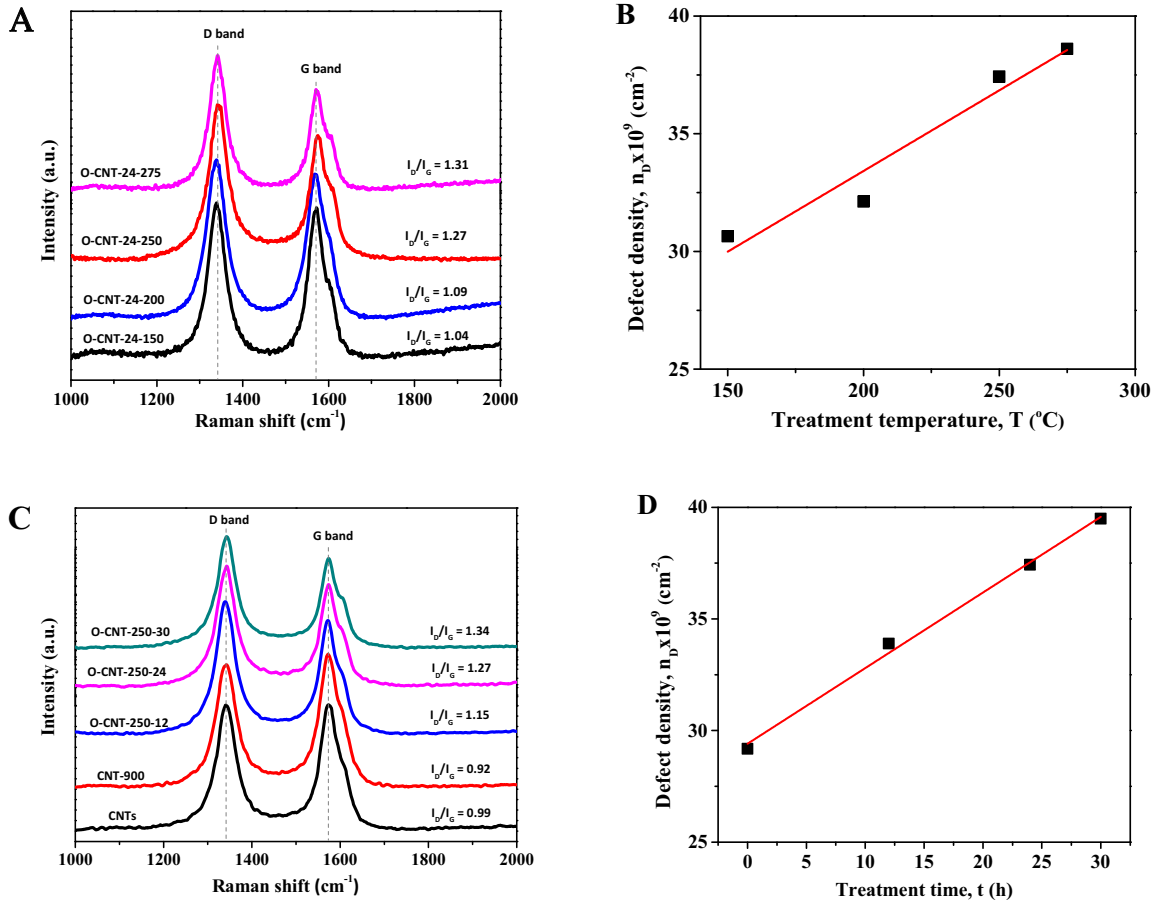

Fig. 1. (A) Raman spectra and I_D/I_G band ratio of the acid treated CNTs materials as a function of the treatment temperature (C) and duration (the temperature was fixed at 250 °C). The Raman spectra of the pristine CNTs and the same after annealing at 900 °C in helium (noted CNT-900) are also reported for comparison. (C and D) Defect density was calculated by Cançado's equation corresponding the I_D/I_G intensity ratio of oxidized CNTs.

severe reaction conditions such as low temperature, high gaseous space velocity and low oxygen-to-reactant molar ratio. However, nitrogen-doping requires the use of nitrogen precursors which are relatively toxic [34–37] and also, the low yield of the doping also leads to a high amount of post-reaction waste to be treated. It is of interest to find other methods to prepare such metal-free catalyst at mild reaction conditions and easy for scale up process. The method should also provide lower waste or even better, waste that can be easily recycled for subsequence use.

Recently, Song et al. [38] reported that the defective MWCNTs is active for benzene hydroxylation to phenol reaction in the presence of H_2O_2. In this study the catalytic performance can be directly correlated with the number of defects on the surface of the CNTs. Another study of Waki et al. [39] also indicated that the defects such as pentagon-heptagon pair and edge plane defects can modify the electronic structure of the carbon allowing an improvement of the oxygen reduction reaction (ORR) performance of the catalyst. The activity performance is mainly attributed to the creation of new active sites on the surface of the oxidized CNTs. Schlögl and co-workers have also reported that prismatic planes of carbon-based material associated with oxygen molecules could efficiently catalyze the oxidation of butane into acrylic acid [40]. Very recently, Wu et al. [41,42] have reported an important role of carbonyl group, which were generated by oxidation process of CNTs using H_2O_2 as gaseous oxidant, in the catalytic reduction of nitrobenzene and nitroarene. According to the results obtained the activity performance of these functionalized CNTs is clearly related to the presence of carbonyl groups present on the surface of the CNTs while the carboxylic group and anhydride played negative roles. However, it is expected that surface oxygen species are mainly linked with the defect sites present on the CNTs surface and thus, the catalytic performance could be originated from such dual sites and not solely to the oxygenated functional groups. A well documented review has recently been published by Collett and McGregor [43] on the catalytic role of carbonaceous deposits in several relevant reactions.

The international restrictions concerning the release of sulfur compounds containing in effluent gas into the atmosphere are becoming more and more drastic during the last decades in order to reduce their disaster environmental footprint [44]. The content of H_2S in crude petroleum, biogas, gas by-products from petroleum refineries and natural gas is significantly different and in general varies from 0.005% up to 90% in volume, respectively. It is also worthy to note that the coal liquefaction process is also considered to be the major source of H_2S emission in the near future [45]. Due to its toxicity, in addition to the corrosion problems that could occur within industrial plants, its removal from gas is crucial before releasing the effluents into atmosphere. A large part of the H_2S was removed via the Claus process [46] while the residual un-reacted H_2S will be converted into elemental sulfur at different reaction temperatures through the selective oxidation, i.e., Super-Claus process [47,48]. Notably, iron- and vanadium-based catalysts have induced a larger amount of research effort in past decades compared with other metal oxide-based catalysts. Iron oxide has relatively high activity for H_2S oxidation [49,50], but its sulfur selectivity is relatively low because of the excess oxygen require-

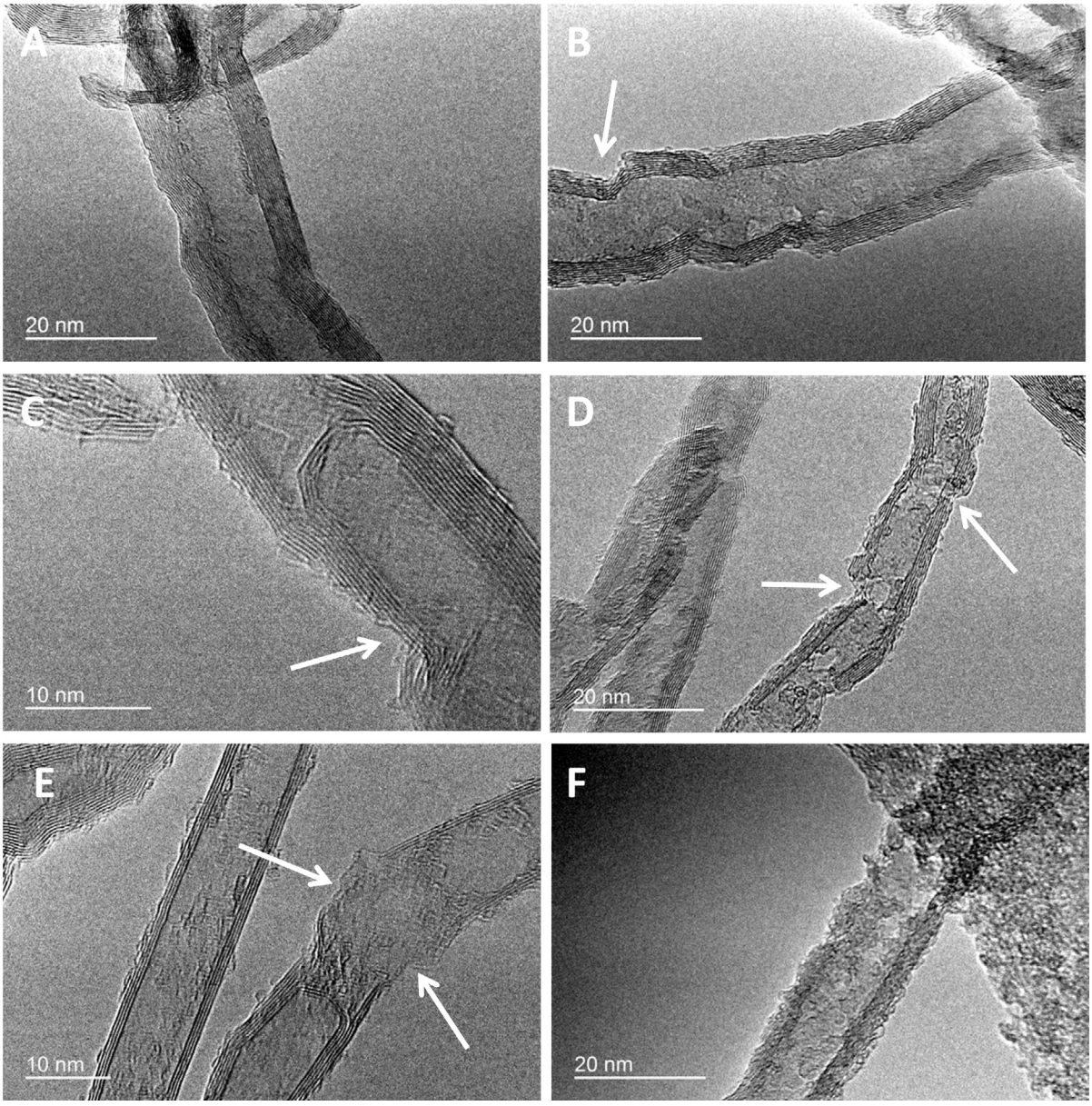

Fig. 2. Representative TEM micrographs of the raw CNTs and the same after an acid treatment at various temperature and duration: (A) Pristine graphitized CNTs, (B) 150 °C for 12 h, (C) 200 °C for 24 h, (D) 250 °C for 24 h, (E) 275 °C for 24 h, and (F) 250 °C for 30 h. Sidewall defects generated during the acid treatment are indicated in the micrographs with arrows.

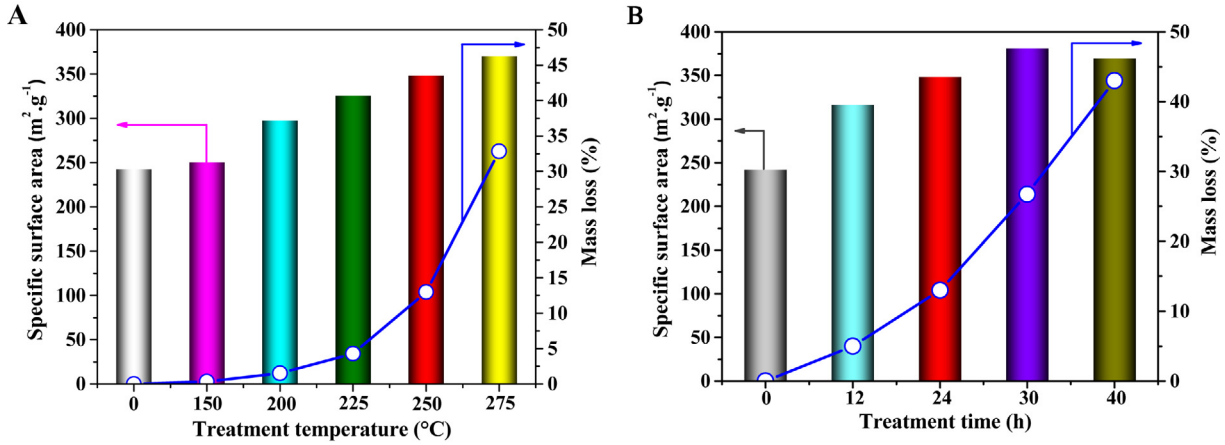

Fig. 3. Weight loss (open circles) and specific surface area (bares) modification of the acid treated carbon-based materials as a function of the treatment temperature with a duration fixed at 24 h (A) and duration at a fixed temperature of 250 °C (B).

ment. However, the selectivity and catalytic performance of the iron-based catalysts were significantly increased with a presence of other metal into the iron oxide structure, especially cerium with a sulfur yield as high as 99% under conditions of GHSV = 21.000 h^{-1}, 1% H_2S, and $O_2/H_2S = 0.5$ [51]. The high catalytic and sulfur selectivity were mainly attributed to the improved redox ability of cerium and the oxygen offered by the cerium lattice. According to the report of Terörde et al. Fe_2O_3/SiO_2 catalysts [52] exhibit excellent activity performance with 97% sulfur selectivity and 94% sulfur yield at 240 °C under the following reaction conditions: 1 vol.% H_2S, 5 vol.% O_2, 30 vol.% H_2O, and balance He. The high catalytic activity can be assigned to the fact that SiO_2 can significantly stabilize the formed iron(II) sulfate species. It is worthy to note that the formation of FeS_2 or iron oxysulfide with high sulfur content due to the H_2S concentration fluctuation is responsible for the catalyst deactivation. On the other hand, various metal oxides such as TiO_2, VO_x loading on SiO_2 were employed. These catalysts also displayed a high desulfurization performance with >92% of H_2S conversion and >90% of sulfur selectivity depending on the reaction temperature. However, for all these catalysts the sulfur selectivity decreased sharply with the further rise of reaction temperature, which probably due to the reaction between the oxygen and sulfur radical on the SiO_2 support surface. Previous works from our laboratory have shown that the Fe_2O_3/SiC catalyst also exhibits a high activity and selective performance for the selective oxidation reaction [53–55]. However, the main drawbacks of these oxide-based catalysts are their high sensitivity to the fluctuation of the H_2S and oxygen concentrations in the mixture as discussed above and sintering which led to a gradual decrease of the catalytic activity.

In the present article we report on the use of gaseous oxidative HNO_3 to create surface defects, with exposed prismatic planes and decorated with oxygen functionalized groups, on the CNTs wall. The oxidized CNTs will be further tested as metal-free catalyst for the selective oxidation of H_2S issued from the refinery stream effluents. The as-treated metal-free catalyst exhibits an extremely high catalytic performance as well as stability compared to the untreated and iron-based catalysts. The catalytic sites could be attributed to the presence of oxygen species such as carbonyl and carboxyl groups decorating the structural defects present on the CNTs surface upon treating under gaseous HNO_3. It is worthy to note that as far as the literature results are concerned no such catalytic study using oxidized CNTs directly as metal-free catalyst has been reported so far.

2. Experimental

2.1. CNTs preparation

The carbon nanotubes were synthesized according to the Chemical Vapor Deposition (CVD) method reported previously [56,57]. The synthesis process is the following: firstly, γ-Al_2O_3 support was impregnated with an aqueous solution containing $Fe(NO_3)_3$ (20 wt.% Fe) by an incipient wetness impregnation method. The as-prepared Fe/Al_2O_3 sample was dried at room-temperature for overnight and oven-dried at 110 °C for 24 h. It was then calcined in air at 350 °C for 2 h in order to transform the nitrate precursor into its corresponding oxide. The Fe_2O_3/Al_2O_3 catalyst was then reduced under hydrogen flow (200 mL/min) at 400 °C for 2 h and then, the reaction temperature was raised to 750 °C (heating rate of 10 °C/min) and the H_2 flow was replaced by a C_2H_6/H_2 mixture to growth the CNTs. The C_2H_6 and H_2 flow rates were fixed at 50:50 sccm min^{-1}. The synthesis was lasted for 3 h, and the reactor was cooled to room temperature under argon.

After synthesis the raw product was treated with a solution of NaOH (20 wt.%) at 110 °C for 24 h in order to remove the alumina support. The resulting material was washed several times with distilled water until neutral pH and then treated with a mixed solution of concentrated HCl and HNO_3 (3/1 vol./vol.) at 110 °C for 17 h in order to remove the remaining iron particles. It was then washed with distilled water until neutral pH and dried at 110 °C.

2.2. Gaseous HNO_3 treatment of CNTs

The as-synthesized pristine CNTs were first thermally treated under argon for 1 h at 900 °C to remove the polyaromatic and amorphous carbon impurities on the surface. For the gaseous acid treatment 1 g of CNTs was loaded inside a tubular reactor (5 × 100 mm) and heated to the desired temperature between 150 °C and 275 °C by an external furnace. The treatment temperature was controlled by a thermocouple inserted inside the furnace. The reactor containing CNTs was connected to a round bottom flask filled with 150 mL of HNO_3 with a concentration of 65%. The temperature of the round bottom flask was fixed at 125 °C and the HNO_3 solution was keep under magnetic stirring. The gaseous acid passed through the CNTs bed was further condensed in another flask which can be re-used for the process. The sample was treated at different temperatures and also with different durations in order to rule out the influence of these treatments on its final microstructure and chemical properties and to correlate these physical properties with the catalytic activity.

2.3. Characterization techniques

The TEM analysis was carried out on a JEOL 2100F working at 200 kV accelerated voltage, equipped with a probe corrector for spherical aberrations, and a point-to-point resolution of 0.2 nm. The sample was grinded into powder and then dispersed by ultrasounds in an ethanol solution for 5 min and a drop of the solution was deposited on a copper grid covered with a holey carbon membrane for observation.

The scanning electron microscopy (SEM) was carried out on a JEOL 2600F with a resolution of 5 nm. The sample was deposited onto a double face graphite tape in order to avoid the problem of charging effect during the analysis.

The Raman analysis was carried out using a LabRAM ARAMIS confocal microscope spectrometer equipped with CCD detector. A laser line was used to excite sample, 532 nm/100 mW (YAG) with Laser Quantum MPC600 PSU.

The specific surface area of the support and the catalyst, after reduction, was determined in a Micromeritics sorptometer. The sample was outgassed at 250 °C under vacuum for 8 h in order to desorb moisture and adsorbed species on its surface.

The X-ray photoelectron spectroscopy (XPS) measurements of the support and catalyst were performed by using a MULTILAB 2000 (THERMO) spectrometer equipped with an AlKα anode ($h\nu$ = 1486.6 eV) with 10 min of acquisition to achieve a good signal to noise ratio. Peak deconvolution was performed with the "Avantage" program from the Thermoelectron Company. The C1s photoelectron binding energy was set at 284.6 ± 0.2 eV relative to the Fermi level and used as reference to calibrate the other peak positions.

2.4. Selective oxidation process

The catalytic selective oxidation of H_2S by oxygen (Eq. (1)) was carried out in an all glass apparatus working isothermally at atmospheric pressure. The temperature was controlled by a K-type thermocouple and a Minicor regulator. The gas mixture was passed downward through the catalyst bed. Before the test, the reactor was flushed with helium at room temperature until no trace of oxygen was detected at the outlet. The helium flow was replaced by the one

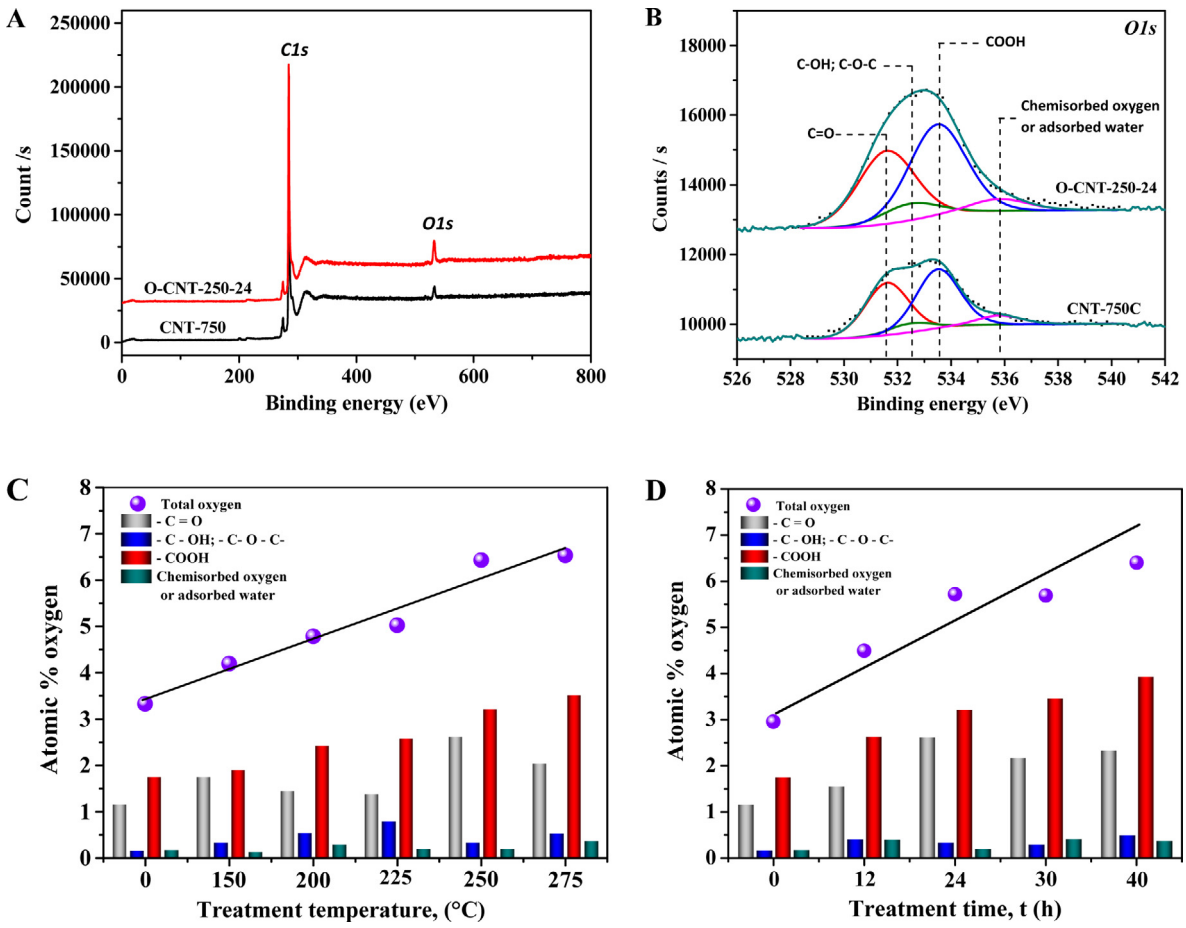

Fig. 4. (A) Survey XPS of O-CNT-250-24 in comparison with pristine graphitized CNTs, (B) Deconvolution O1s present the oxygen species on the surface of the CNTs wall, (C and D) Oxygen species distribution of the acid treated carbon-based materials as a function of the treatment duration and temperature in comparison with the pristine graphitized CNTs.

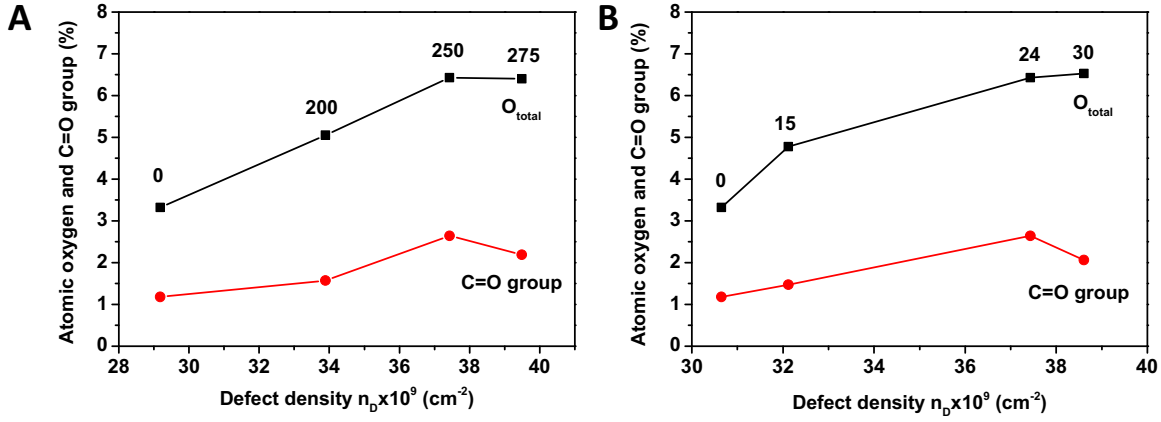

Fig. 5. (A) Amount of incorporated total oxygen and carbonyl group as a function of defect density generated during the acid treatment temperature and duration. The treatment duration is keep at 24 h. (B) Amount of incorporated oxygen and defect density as a function of the acid treatment duration. The treatment temperature is keep at 250 °C. The relative error margin is amounted to 0.5% for the O_{total} taken into account the uncertainty of the XPS analysis and 1% for the C=O groups.

containing steam. The catalyst was slowly heated up to the reaction temperature, and then the wet helium flow was replaced by the reactant mixture. The gases (H_2S, O_2, He) flow rate was monitored by Brooks 5850TR mass flow controllers linked to a control unit. The composition of the reactant feed was H_2S (1 vol.%), O_2 (0.63 vol.%, 1.25 vol.% or 2.5 vol.%), H_2O (30 vol.%) and He (balance). The use of a relatively high concentration of steam in the feed is motivated by the will to be as close as possible to the industrial working conditions as the steam formed during the former Claus units is not removed before the oxidation step and remains in the treated tail gas. The steam (30 vol.%) was fed to the gas mixture by bubbling a helium flow through a liquid tank containing water maintained at 85 °C. The O_2-to-H_2S molar ratio was varied from 0.63 to 2.5 with a WHSV fixed at 0.6 h^{-1}. It is worth to note that the WHSV used in the present work is extremely high regarding the usual WHSV

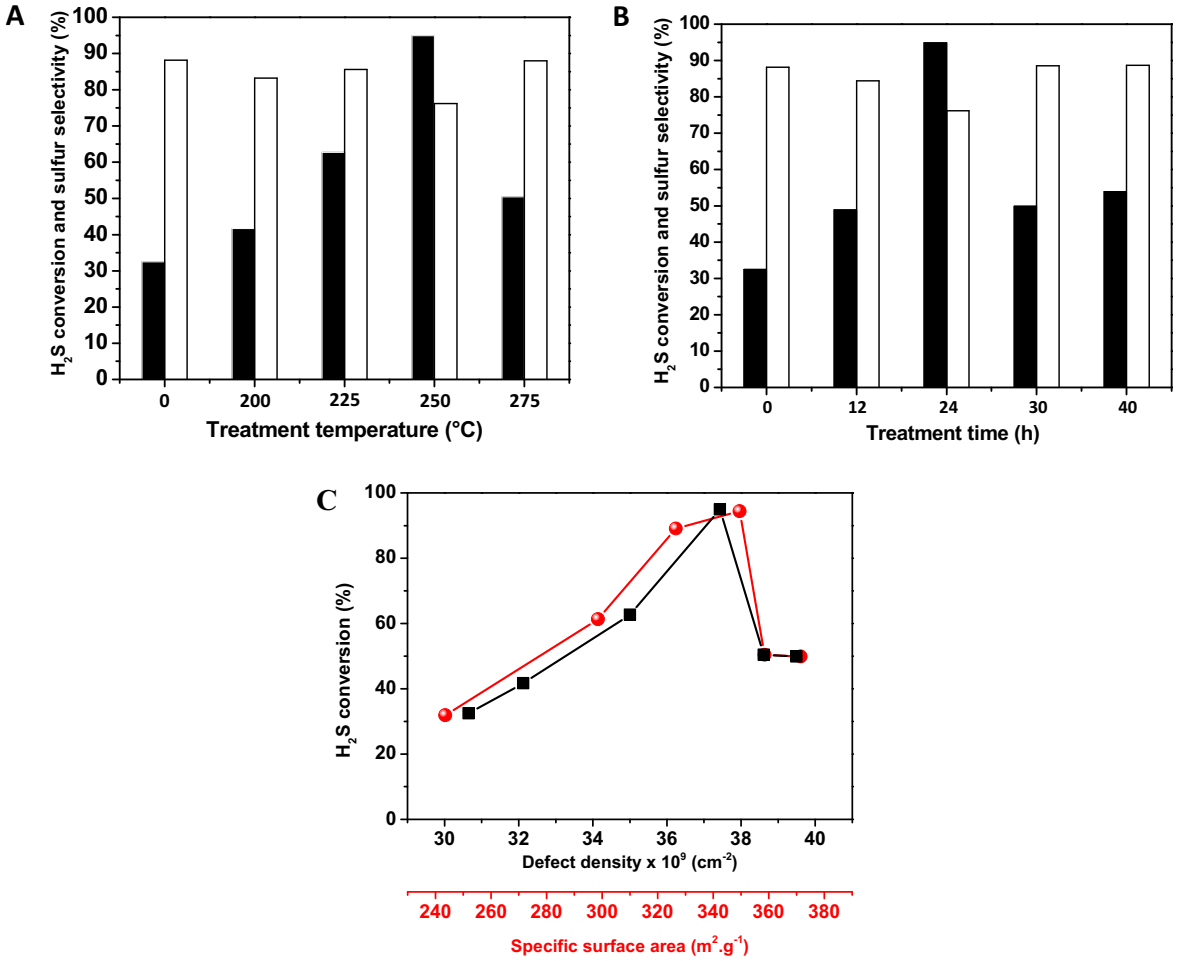

Fig. 6. (A and B) Desulfurization activity on the O-CNT catalysts treated at different temperatures and durations under gaseous HNO_3. Black bar: H_2S conversion, White bar: sulfur selectivity. (C) H_2S conversion and sulfur yield of O-CNTs catalysts as function of the defect density and surface specific area. Reaction conditions: catalyst weight = 0.3 g; reaction temperature = 230 °C; WHSV = 0.6 h^{-1}; O_2-to-H_2S molar ratio = 2.5.

used in the industrial process for this kind of reaction, i.e., 0.09 h^{-1} (GHSV: 1500 h^{-1}).

$$H_2S + ½O_2 \rightarrow 1/nS_n + H_2O \qquad \Delta H = -222\ kJ\ mol^{-1} \qquad (1)$$

The reaction was conducted in a continuous mode and the sulfur formed during the reaction was vaporized, due to the relatively high partial pressure of sulfur at these reaction temperatures, and was further condensed at the exit of the reactor in a trap maintained at room temperature.

The analysis of the inlet and outlet gases was performed on-line using a Varian CP-3800 gas chromatography (GC) equipped with a Chrompack CP-SilicaPLOT capillary column coupled with a thermal catharometer detector (TCD), allowing the detection of O_2, H_2S, H_2O and SO_2.

3. Results and discussion

3.1. Characteristics of the acid treated CNTs

In this work, the CNTs after acid treated are noted as follows: O-CNT-(X), for the treatment temperature, and -(Y), for the treatment duration in hour, for example: O-CNT-250-24 indicates that the raw CNTs were treated at 250 °C for 24 h under gaseous HNO_3. The Raman spectra of the different samples obtained as a function of the treatment temperature and duration are presented in Fig. 1A and C. Raman spectra of all samples display two peaks localized at 1343 cm^{-1} (D-band) and 1573 cm^{-1} (G-band). The G-band corresponds to the sp^2 carbon atoms in the graphene sidewalls, while the D-band was attributed to the structural defects and partially disordered structures of the sp^2 domains [16,56].

The I_D/I_G intensity ratio was used to estimate the amount of defects in the tubes. The I_D/I_G intensity ratio of oxidized CNTs as a functional of treatment temperature and duration are presented in Fig. 1A and C. According to the Raman results, increasing the acid treatment temperature and duration leads to an increase of the I_D/I_G ratio which indicates that more defects have been incorporated inside the CNTs structure.

The defects density can be also calculated from the D'-band localized at around 1610 cm^{-1}. The deconvoluted results show the increase of the contribution of the D'-band as increasing the temperature and duration of the gaseous HNO_3 treatment which again confirms the formation of defects within the acid treated tubes. Indeed, the D'-band percent increases from 4 to almost 8.6% after an acid treatment at 250 °C for different durations. Similar results were also observed with the acid treated samples as a function of the temperature.

In order to confirm such tendency the amount of defect density was calculated from the Raman data. Cançado et al. [58] have proposed an empirical equation to calculate the amount of defect

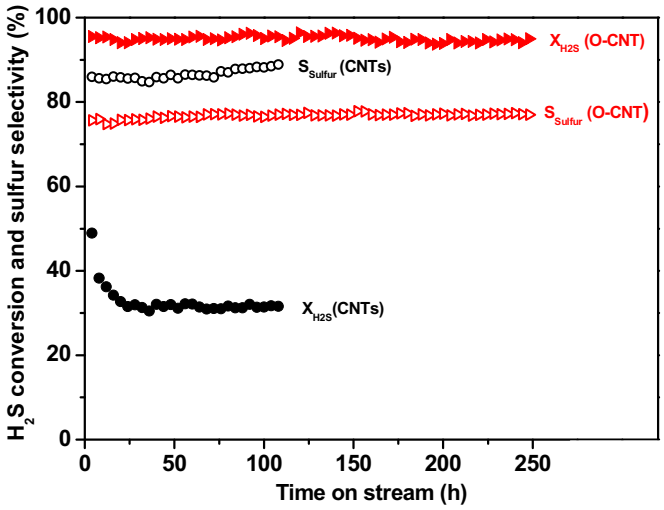

Fig. 7. Desulfurization conversion, sulfur selectivity on the O-CNT-250-24 (O-CNT) compared to the CNT graphitized at 750 °C (CNT). Reaction conditions: catalyst weight = 0.3 g; reaction temperature = 230 °C; steam = 30%, WHSV = 0.6 h^{-1}; [H_2S] = 1%, O_2-to-H_2S molar ratio = 2.5. Notation: X_{H2S}: H_2S conversion, S_{Sulfur}: sulfur selectivity.

density n_D (cm^{-2}) on the surface of the CNTs based on the Raman data (Eq. (2)):

$$n_D = (7.3 \pm 2.2) \times 10^9 E_L^4 \left(\frac{I_D}{I_G}\right) \quad (2)$$

where E_L is the terms of excitation energies and I_D and I_G are the intensity of the Raman spectrum. In this work the excitation energies was fixed at 2.33 eV.

The density of defects (n_D), determined on the different samples according to Cançado's equation, are presented in Fig. 1B and D. Such results clearly indicate that increasing the severity of the acid treatment, i.e., temperature or duration, leads to a monotonous increase of the defects inside the carbon nanotubes compared to the pristine CNT after carbonization step. Thus, the defect density is directly linked with the acid treatment conditions and the role of these defects to mediate desulfurization process will be discussed in light of the catalytic results presented below. According to the results, the defects density can be also easily controlled by adjusting the treatment parameters according to the results presented above. The sample after treatment was washed with distilled water and oven-dried at 110 °C for overnight. The main advantage of the process is that the treated sample can be directly used without any needs for post-activation treatment such as filtering and acid neutralization as usually needed.

The microstructure of the CNTs, after annealing step, and after acid treatment under various conditions, is analyzed by TEM and the results are presented in Fig. 2. TEM micrograph of the carbonized CNTs evidences the high graphitized microstructure of the tube along with the presence of a thin layer of amorphous carbon on the outer wall (Fig. 2A). The amorphous carbon presence on the tube surface could be formed during the cooling process under the presence of the reactant mixture. Indeed, it is expected that at temperature lower than the synthesis one some hydrocarbon can still be decomposed leading to the formation of amorphous carbon instead of CNTs due to the insufficient growth temperature [59]. Apparently, the carbonization treatment at 900 °C is not sufficient to remove all the amorphous carbon present on the tube wall. The selectivity towards the CNTs formation is extremely high under the used reaction conditions as no carbon nanoparticles were observed within the sample. TEM analysis also evidences the complete removal of the iron growth catalyst inside the sample and allows one to rule out the role of residual iron catalyst in the partial oxidation process.

The acid treatment leads to a significant structural modification of the CNTs according to the TEM analysis. At low acid treatment temperature (≤250 °C) or with a short treatment time (≤24 h), the TEM micrographs evidence the formation of structural nanoscopic defects on the tube wall (Fig. 2B–D) while the main shape of the tube remains unmodified. The observed defects formed on the tube wall after the acid treatment could be attributed to the specific attack by the gaseous HNO_3 of the vacancies or pentagon-heptagon pairs with high reactivity in the tube wall. At higher acid treatment temperature and longer duration a significant modification of the CNTs structure is observed. Indeed, at higher treatment temperature (>250 °C) and higher duration (>24 h) a significant part of the tubes was destroyed according to the TEM micrographs recorded on the O-CNT-275-24 (Fig. 2E) and O-CNT-250-30 (Fig. 2F).

These results are in good agreement with those of the Raman analysis presented above which clearly evidence an increasing of the defects density as increasing the severity of the acid treatment process. Similar results have also reported by other research groups during their investigations on the influence of the gaseous acid treatment on the CNTs integrity [16,56]. Recently, Zhou et al. [60] also reported the formation of defects on the CNTs wall even after a mild treatment in the presence of HNO_3.

The formation of defects along the tube wall during the acid treatment step also significantly increases the overall specific surface area of the as-treated materials. The specific surface area of the acid treated CNT steadily increased as a function of the acid treatment temperature and duration as evidenced in Fig. 3A and B. The specific surface area of the O-CNT-250-24 and O-CNT-275-24 are 1.6 times higher than that of the graphitized CNT, i.e., 371 and 382 m^2/g instead of 243 m^2/g. According to the results in Fig. 3B, the specific surface area of the acid treated CNT reached a maximum after 30 h of treatment at 250 °C. The increase of the specific surface area of the treated samples could be directly attributed to the creation of defects on the tube wall leading to a higher adsorption sites for nitrogen. However, at higher treatment duration the specific surface is decreased and such result could be assigned to the destruction of the tubes morphology or to the formation of disordered carbon phase with low specific surface area.

The gaseous acid treatment also induces an overall oxidation of carbon matrix leading to a significant weight loss of the treated material. Such phenomenon has already been reported by Xia and co-workers with a similar treatment [19] and also by several groups in the literature [15,20]. The weight loss during the acid treatment process is accounted for the corrosion of the tubes, and also to the removal of amorphous carbon layer presence on the tube wall and some carbon encapsulated residual growth catalyst; this later is expected to be relatively low taken into account the initial weight amount of the growth catalyst in the final composite. The weight loss calculated on the basis of the initial weight and the one after acid treatment as a function of the treatment duration and temperature is presented in Fig. 3A and B.

The weight loss increases with the treatment temperature and duration, especially for temperature >225 °C or duration longer than 24 h. It is expected that the low temperature weight loss could be assigned to the removal of the amorphous carbon or catalyst residue, since they are considered to be more reactive than the graphitic wall of the carbon nanotubes while at high temperature, weight loss is linked with the removal of carbon in the graphitic structure consecutive to the formation of structural defects on the tube wall. Indeed, under a more severe treatment, i.e., longer duration or higher temperature, the weight loss becomes significantly, i.e., the weight loss recorded for the sample after being treated at 275 °C for 24 h and 40 h are 33% and 43%, respectively. This result

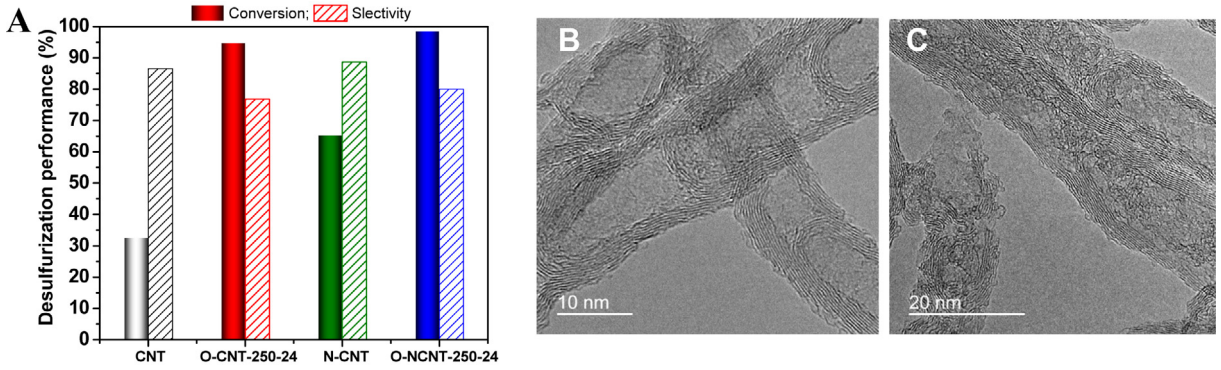

Fig. 8. (A) Desulfurization performance on the pristine CNTs and N-CNTs catalysts and the same after acid treatment at 250 °C for 24 h. Reaction conditions: catalyst weight = 0.3 g; reaction temperature = 230 °C; [Steam] = 30%, [H_2S] = 1%, O_2-to-H_2S = 2.5, WHSV = 0.6 h^{-1}. (B and C) Corresponding TEM micrographs of the N-CNTs and CNTs after acid treatment at 250 °C for 24 h.

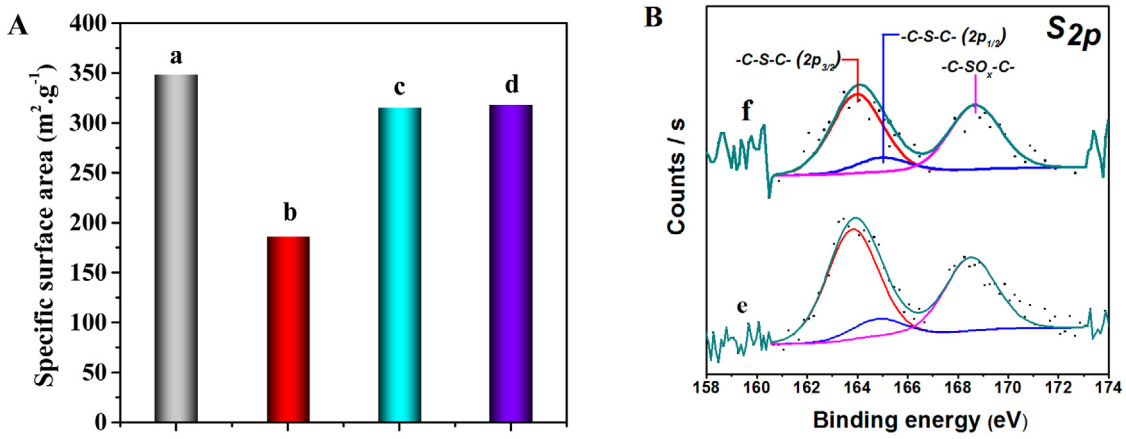

Fig. 9. (A) Specific surface area of O-CNT-250-24 catalyst before (a)—after desulfurization test (b) and after thermal regeneration under helium flow at different temperatures: 320 °C (c) and 450 °C (d) for 2 h. (B) XPS S_{2p} spectra on catalyst surface after about 300 h of desulfurization test (e) and after thermal regeneration under helium flow at 450 °C for 2 h (f).

can be attributed to the higher corrosion of the tubes wall and also to the tube breaking according to the TEM analysis presented above.

The amount of the oxygen engaged in the different oxygenated functional groups is analyzed by means of the XPS technique and the results are presented in Fig. 4. According to the XPS survey spectra recorded on the pristine graphitized CNTs and the same after gaseous acid treatment at 250 °C for 24 h no change has been observed and only C1s and O1s peaks are observed (Fig. 4A). The deconvoluted O1s spectrum in Fig. 4B shows the presence of four peaks which can be assigned to the =C=O (ketone, aldehyde, quinone. . .), —C—OH, —C—O—C— (alcohol, ether) and—O—C=O (carboxylic, ester) oxygen species [20]. According to the XPS results presented in Fig. 4C and D the acid treatment leads to a significant increase of the total amount of oxygen from 3.5 to about 6 at.%. The oxygen engaged in the different functional groups steadily increases as increasing the treatment temperature and treatment duration while the chemisorbed oxygen and/or adsorbed water remain virtually unchanged.

In Fig. 5 the atomic percent of total incorporated oxygen and carbonyl groups inside the CNT versus the density defects, as a function of the treatment temperature (Fig. 5A) and duration (Fig. 5B), are presented. According to these results the total oxygen and carbonyl group concentration is proportional to the amount of defect density which increase almost linearly with the acid treatment temperature up to 250 °C and duration of 24 h. Higher treatment temperature, i.e., 275 °C, or longer treatment duration, i.e., >24 h at 250 °C, lead to an almost unchanged values of the total incorporated oxygen and defects density while the amount of the C=O group decrease. The high temperature and duration treatment also lead to the significant damaging of the tube morphology according to the TEM analysis presented above. According to the results one can stated that the optimized treatment conditions are 250 °C for 24 h, which allow one to tailor O-CNTs with a highest amount of oxygen, defects and specific surface area without significant tube damage or breaking for subsequence catalytic applications.

3.2. Selective oxidation of H_2S

In order to assess in detail the role of defect sites and/or oxygenated functional groups on the desulfurization performance of the acid treated CNTs, desulfurization tests were carried out on the different catalysts activated at different temperatures and durations and the catalytic results are presented in Fig. 6. All the desulfurization tests were carried out for at least 30 h and the average desulfurization performance is reported. According to the results the acid treatment process leads to the formation of active metal-free catalysts for desulfurization reaction compared to the pristine graphitized CNTs (Fig. 6A and B). The CNTs treated during 24 h at 250 °C displays the highest desulfurization performance among the tested catalysts. The results obtained also indicate that both H_2S conversion and sulfur yield increase as a function of the defect density (n_D) and specific surface area (Fig. 6C), for the samples treated at a temperature lower than 250 °C or with a duration shorter than 25 h.

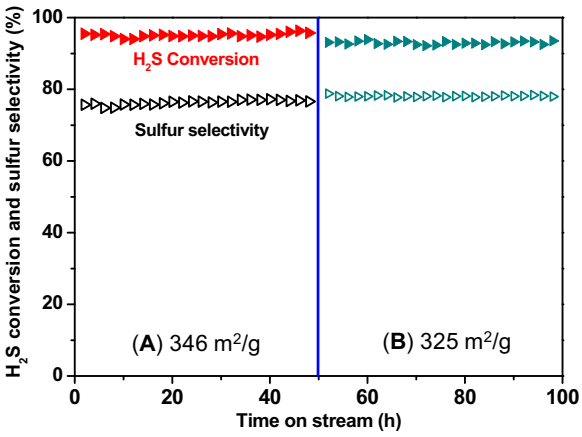

Fig. 10. Desulfurization activity, expressed in terms of H_2S conversion and sulfur selectivity, on the O-CNT-250-24 before (A) and after thermal treatment under helium at 450 °C for 2 h (B). Reaction conditions: catalyst weight = 0.3 g; reaction temperature = 230 °C; WHSV = 0.6 h^{-1}, [Steam] = 30%, [H_2S] = 1%, O_2-to-H_2S = 2.5.

According to the obtained results, the increase of the desulfurization activity, expressed in terms of H_2S conversion, could be attributed to the high defect sites present on the tube wall which could play a role of adsorption center for the reactants. It is expected that strain and oxygen atoms present in the defects could strongly participate to the stabilization of these later for subsequence catalytic process. These local interactions allow the maintenance of these high energy sites during the course of the reaction. The improved desulfurization performance could also be attributed to the present of oxygenated functional groups, on or around these high energy defect sites present on the surface of the CNTs after acid treatment as advanced above. Among these different oxygenated functional groups, the carbonyl group seems to be the most important, while the other group such as carboxylic and anhydride played negative roles for selective oxidation of H_2S according to the results reported by Su and co-workers [41,42] on the oxygen-treated CNTs for the hydrogenation of arenes. The results reported in Fig. 4C and D evidence that on the catalysts treated under severe conditions, i.e., longer duration or at higher temperature, both the carboxylic groups and total amount of oxygen still increase while the desulfurization activity decreased (Fig. 6A and B). However, it is worthy note that the CNTs morphology was drastically changed at these treatment conditions due to the excessive oxidation and thus, could be at the origin of the loss of the catalytic performance. The high open porous structure of the O-CNT catalyst, which provides a high effective surface contact between the reactant and the active sites compared to the CNTs graphitized, also represents a net advantage for performing the catalytic reaction.

In heterogeneous catalysis the adsorption of the reactants and desorption of intermediate product govern the kinetics of the process. If the desorption rate is somewhat lowered, i.e., strong interaction of the product with the active center or rapid re-adsorption on adjacent active centers, the secondary reaction will be favored and thus leading to the formation of thermodynamic product. The decreasing of the sulfur selectivity compared to that obtained on the CNT graphitized ones could be attributed to the presence of adjacent prismatic planes in the defect which could bind stronger the intermediate sulfur species leading to a secondary total oxidation process to yield SO_2 [22]. The sulfur selectivity lost could also be partly attributed to the high H_2S conversion on the metal-free oxygen treated catalysts. Both of these hypotheses will be evaluated and discussed later on.

The long term desulfurization test was carried out under the optimum reaction conditions that we have reported in previous articles [22–24], i.e., 230 °C and with a WHSV fixed at 0.6 h^{-1}, on the graphitized CNT and the same after an acid treatment, O-CNT-250-24. The desulfurization results as a function of time on stream are presented in Fig. 7. According to the results, the desulfurization performance of the acid treated O-CNT-250-24 catalyst displays a significant improvement compared to the graphitized CNT catalyst, i.e., conversion of 95% instead of 32%, under the same reaction conditions. No deactivation was observed on both catalysts as a function of time on stream which indicates the high resistance of the catalysts towards active phase loss by both sintering and surface blocking. The low desulfurization activity observed on the graphitized CNTs could be attributed to the low defects on the tube wall compared to the O-CNTs. In contrast, the O-CNT-250-24 exhibits slightly lower sulfur selectivity compared to that obtained on the CNT graphitized, i.e., 75 instead of 85%. Such lower sulfur selectivity could be attributed to the high desulfurization activity or to the re-adsorption of the intermediate sulfur species on the oxygenated defects sites followed by secondary reaction leading to the formation of SO_2 product. The desulfurization results obtained clearly showed that the catalytic performance of the CNTs catalyst is strongly improved after an acid treatment process which introduces both oxygen functionalized groups and defects density on the catalyst surface.

Table 1
The desulfurization performance over O-CNT-250-24 catalyst under different reaction conditions.

	X_{H2S} (%)	S_S (%)	S_{Yield} (%)
Influence of the reaction temperature (WHSV = 0.6 h^{-1}, O_2-to-H_2S = 2.5)			
230 °C	95	76	72.2
210 °C	80	88	70.4
190 °C	50	90	45.0
Influence of the gas velocity (T = 230 °C, O_2-to-H_2S = 2.5)			
0.6 h^{-1}	95	76	72.2
0.9 h^{-1}	90	80	72.0
1.2 h^{-1}	85	85	72.3
Influence of the O_2-to-H_2S ratio (WHSV = 0.6 h^{-1}, T = 230 °C)			
2.5	95	76	72.2
1.2	90	80	72.0
0.63	85	85	72.3

Notes: X_{H2S}: H_2S conversion, S_S: sulfur selectivity; S_{Yield}: sulfur yield.

The H_2S conversion on the O-CNT-250-24 has also been lowered in order to check out if the low sulfur selectivity is belonging to the high conversion of the catalyst. Some improvement of the sulfur selectivity was observed at low H_2S conversion (Table 1), indeed, the sulfur selectivity rise up to about 90% when the H_2S conversion is lowered to 50%. Such result indicates that in order to assume high H_2S conversion per pass an optimization process is needed to improve the sulfur selectivity. Indeed, according to the catalytic results one can stated that the sulfur selectivity remains relatively low on the O-CNT catalyst. Such low sulfur selectivity could be attributed to the high adsorption strength of either the H_2S or sulfur on the active sites.

The O-CNT-250-24 catalyst is further evaluated under different reaction conditions in order to map out the influence of the structural defects and the oxygenated functionalities on the desulfurization performance and stability. The results obtained under different reaction conditions are summarized in Table 1.

The effect of the reaction temperature on the desulfurization performance of the O-CNT-250-24 catalyst was performed with the WHSV fixed at 0.6 h^{-1} and the O_2-to-H_2S molar ratio at 2.5. The catalyst was evaluated first at 230 °C for 40 h of test and then the reaction temperature was lowered to 210 °C and 190 °C for subsequently 30 h of test, respectively. According to the results presented in Table 1 the H_2S conversion decreases as decreasing the reaction temperature while the sulfur selectivity increase in a reverse way. However, at 190 °C the H_2S conversion loss is more pronounced while the sulfur selectivity remains almost unchanged at 90%. Such

result could be explained by the fact that the sulfur selectivity observed under these reaction conditions represents the intrinsic selectivity towards sulfur on the OCNT-250-24 catalyst and thus, cannot be improved due to the rate of re-adsorption and secondary oxidation.

The desulfurization test was also realized as a function of the weight hourly space velocity, i.e., at 0.6, 0.9 and 1.2 h^{-1}, at 230 °C and an O_2-to-H_2S ratio of 2.5 and the results obtained are summarized in Table 1. According to the results the O-CNT-250-24 displays a relatively high H_2S conversion even at high space velocity, i.e., 85% at 1.2 h^{-1}. Such a high desulfurization performance could be attributed to the high effective surface area and surface exposure active sites of the catalyst which significantly enhance the reactant adsorption. The high space velocity also leads to an improvement of the sulfur selectivity, up to 85%, due to the high escaping rate of the intermediate sulfur from the active site.

The influence of the O_2-to-H_2S molar ratio on the desulfurization performance was also studied in order to confirm the high activity of the O-CNT to generate active oxygen species for oxidizing H_2S compounds. The results obtained at different O_2-to-H_2S molar ratios, i.e., 2.5, 1.25 and 0.63, as a function of time on stream are summarized in Table 1. The decreasing of the O_2-to-H_2S ratio led to a monotonous decrease of the H_2S conversion, however, this later remains very high (about 85%) even at the lowest O_2-to-H_2S ratio at 0.63 and under a relatively high space velocity (0.6 h^{-1}). The catalyst also exhibits an extremely high stability for all the reaction conditions which indicates that deactivation by removal of the oxygenated functional groups on the catalyst surface is negligible. The explanation is that those oxygenated groups were introduced into the catalyst at higher temperature treatment and thus, remain stable under the reaction conditions employed. Such stability is of extreme interest for the process as traditional iron-based catalysts are highly sensitive to the H_2S and O_2 fluctuations inside the reactant feed. Indeed, the fluctuation of H_2S in the feed leads to the formation of FeS_2 and iron sulfate species which are less active for the reaction [51–61,62].

On the other hand, the sulfur selectivity slightly increased as decreasing the O_2-to-H_2S ratio due to the lower oxygen available for oxidizing the formed sulfur. These results indicated that the O-CNT catalyst exhibits a high activity for oxygen dissociation which provides enough oxygen to perform the selective oxidation of H_2S even at low oxygen concentration in the reactant mixture and under a relatively high space velocity. The sulfur selectivity of about 85% was obtained at an O_2-to-H_2S ratio of 0.6. Such sulfur selectivity is among the highest value that one can obtain on the acid treated catalyst due to the consecutive reaction between the re-adsorbed sulfur and the excess oxygen in the feed. Similar results have also been observed during the study about the influence of the reaction temperature and space velocity reported above.

The results obtained above clearly indicate that the oxygenated functionalized and defects introduced by the gaseous acid treatment can act as hybrid metal-free sites for the oxidation of H_2S into elemental sulfur similarly to what was observed on the nitrogen-doped carbon nanotubes (N-CNTs) [42]. In order to confirm if the presence of nitrogen doping could have any additional influence on the overall desulfurization performance the same acid treatment was applied for the N-CNTs sample. The N-CNTs synthesized according to our previous report [44] were treated under the same conditions as those used for the CNTs and the catalyst was further evaluated in the selective oxidation of H_2S under the same reaction conditions and the results are presented in Fig. 8. The pristine CNTs catalyst exhibits a relatively low desulfurization performance, i.e., 32%, while the same, after being treated in an aqueous solution of HNO_3 (65 vol.%), exhibits a significant improved desulfurization activity which could be attributed to the dissociative adsorption of oxygen on the prismatic planes present at the defects of the CNTs. Similar results have also been reported by Schlögl and co-workers [40] during the selective oxidation of *n*-butane into acrylic acid on CNTs catalysts. The introduction of nitrogen into the carbon matrix leads to a significant improvement of the desulfurization activity compared to the un-doped CNTs. The presence of nitrogen doping leads to an increase of the H_2S conversion from 32 to 65% under similar reaction conditions. Such results confirm the catalytic role of nitrogen doping in the desulfurization performance of the metal-free catalyst as already been reported previously [24].

The desulfurization performance, expressed in terms of H_2S conversion, of the N-CNTs, after a treatment by a gaseous HNO_3 at 250 °C and 24 h, is significantly increased confirming the important role of oxygenated decorating defects generated by the treatment on the catalytic performance. According to the results the desulfurization activity is almost similar between the O-CNT and the O-N-CNT catalysts, i.e., 95 instead of 97% of H_2S conversion, while the sulfur selectivity is somewhat slightly higher on the O-N-CNT catalysts. The results obtained indicate that metal-free catalysts performance can be tuned either by introducing defects with oxygenated groups or doping with heteroatoms.

3.3. Characteristics of the spent catalysts

The specific surface area (SSA) of the spent O-CNT250-24 catalyst, measured after more than 300 h of reaction, under different reaction conditions, is about 1.7 times lower than that of the fresh catalyst, i.e., 187 instead of 346 m^2/g, as presented in Fig. 9A. It is worthy to note that despite the significant decrease of the overall SSA the desulfurization remains unchanged. Such result could be attributed to the deposition of some solid sulfur with low specific surface area within the catalysts porosity which lowering of the overall specific surface area of the catalysts without any significant modification of the density of the active sites. In order to verify such hypothesis regeneration was performed on the spent catalyst by submitting it to a thermal treatment under helium at 320 °C and 450 °C for 2 h to vaporize the trapped sulfur [22]. After the thermal treatment the catalyst specific surface area was almost recovered which confirming the hypothesis advanced above about the role of solid sulfur in the decrease of the catalyst SSA.

The XPS analysis carried out on the spent catalyst, after more than 300 h on stream, evidences the presence of some sulfur species. The $S2p_{3/2}$ (163.8 eV) and $S2p_{1/2}$ (164.8 eV) peaks are ascribed to sulphide groups (—C—S—C) and the C—SO_x—C peak (168.5 eV) is also observed as displayed in Fig. 9B and summarized in Table 2.

Such sulfur deposition was attributed to the possible deposition of the formed sulfur within the tube channel according to the explanation advanced above. It is expected that the thermal treatment under helium at high temperature allows the removing of a significant part of the deposit sulfur from the catalyst porosity. However, according to the XPS results, there is still 0.44 at.% of sulfur species present on the sample after thermal treatment at 450 °C (about 50% of the sulfur present on the spent catalyst surface). This result indicates that during the treatment part of the deposited sulfur could incorporate into the CNTs network or remain trapped inside the carbon nanotubes channel. However, this residual solid sulfur seems not to influence in a noticeable way the desulfurization activity as no deactivation was observed which again confirm that it is mostly deposited inside the tube channel.

The influence of the regeneration step on the desulfurization performance was investigated and the results are presented in Fig. 10. According to the catalytic results the desulfurization performance, expressed in terms of H_2S conversion, as well as the sulfur selectivity remain almost unchanged (Fig. 10 right) compared to the unregenerate one (Fig. 10 left) which indicate that the deposit sulfur hardly influences the desulfurization performance and partly

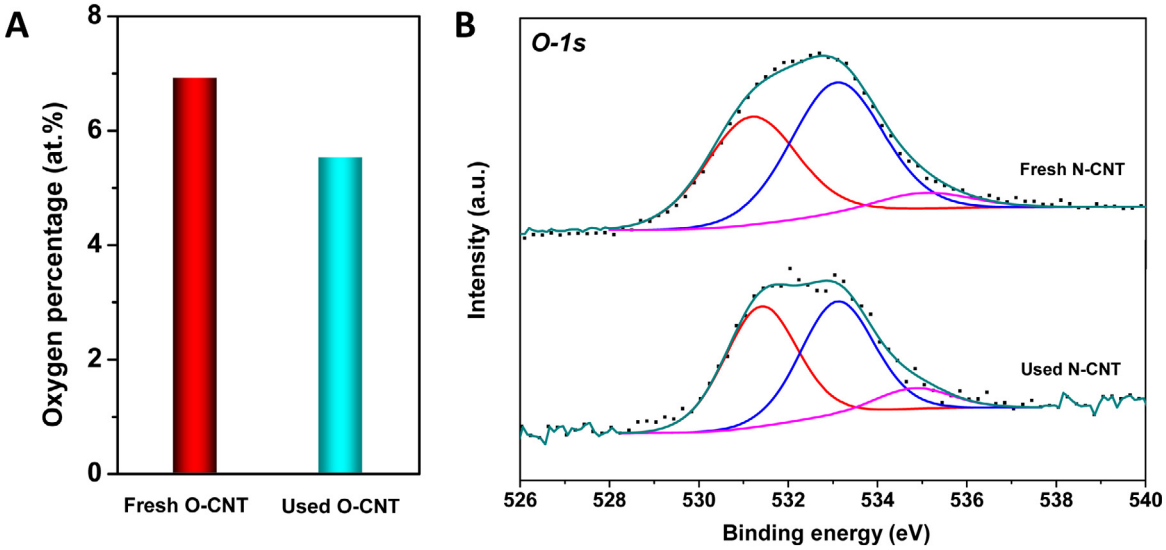

Fig. 11. *O1s* XPS spectra recorded on the O-CNT, before and after desulfurization reaction at various temperatures.

Table 2
The atomic percentage and sulfur species percentages of spent catalyst obtained by XPS after reaction oxidation of H_2S in comparison with that obtained before test.

Samples	C	O	S	-C-S-C-S ($Sp_{3/2}$)	-C-S-C-S ($Sp_{1/2}$)	-C-S_{ox}-C-
O-CNT-250-24	93.32	6.68	–	–	–	–
O-CNT-250-24-OS (*)	94.25	4.97	0.79	0.43	0.07	0.29
O-CNT-250-24-R320 (**)	95.37	4.09	0.56	0.22	0.20	0.14
O-CNT-250-24-R450 (***)	95.49	4.08	0.44	0.17	0.18	0.09

Notes: (*) O-CNT-250-24 catalyst after 300 h of oxidation of H_2S test, (**) O-CNT-250-24 catalyst after 300 h of oxidation of H_2S test and regeneration at 320 °C for 2 h under He flow, (***) O-CNT-250-24 catalyst after 300 h of oxidation of H_2S test and regeneration at 450 °C for 2 h under He flow.

confirm the above mentioned hypothesis that most of the sulfur is localized inside the tube channel allowing the maintain of the active sites and is not actively involved in the catalytic process itself.

3.4. Influence of the defects decorated with oxygen functional groups on the desulfurization performance

The treatment of the CNTs by a gaseous nitric acid had induced the formation of a large number of microstructural defects on the tube wall along with the incorporation of oxygen functional groups on the carbon nanotubes surface, probably next or on the defect sites, according to the characterization results. In addition, the formation of the defects on the tube wall also greatly contributes to an enhancement of the material specific surface area which provides high effective surface contact for the reactants. The efficiency of the acid treatment process can be controlled through the treatment temperature and process duration in order to finely tune the density of the defects on the tube wall without destroying the tube morphology. The optimized treatment conditions were determined: treatment temperature of 250 °C along with duration of 24 h. After such treatment, the nanotubes were decorated with defects along the tube wall but still keep the integrity of the structure. A combination of catalytic results and surface characterization by XPS indicates that both the oxygenated functional groups and the nanoscopic defects generated along the tube wall, with exposed prismatic planes, are mostly responsible for the observed metal-free activity in the desulfurization process. However, it is worthy to note that in the present case the geometry localization of the active centers is not easy defined due to the similar nature with the support. Indeed, in the O-CNT metal-free catalyst it is almost impossible to make a clear partition between the carbon atoms which play a role of support and those acting as active centers in the catalytic process, i.e., "non-innocent support" [63,64] and thus, part of the observed catalytic activity could also come from the underneath carbon atoms as well.

The as-synthesized O-CNT-250-24 catalyst exhibits an extremely high and stable catalytic activity in the selective oxidation of H_2S into elemental sulfur in a fixed-bed reactor. Such high catalytic stability could be attributed to the stability of the defects on the tube wall at the reaction temperature. On the other hand, the present of defects also lead to a rapid re-adsorption of the intermediate sulfur and thus, the secondary reaction leading to the formation of SO_2 is not negligible and was accounted to about 15% of the overall sulfur selectivity. The catalyst also exhibits a high stability as a function of the gaseous space velocity and O_2-to-H_2S ratio indicating the outstanding properties of the defects for performing partial oxidation process. The high stability as a function of the O_2-to-H_2S ratio could be attributed to the lack of any metallic and oxides phases in the catalyst which are more sensitive toward sulfidation as increasing the H_2S concentration in the reactant feed.

It is also worthy to note that the desulfurization performance remains stable despite the presence of some solid sulfur deposited during the course of the reaction which significantly decreases the catalyst specific surface area from 350 to 187 m^2/g. It is expected that such solid sulfur is mostly deposited on the intact wall or inside the inner channel of the tube with higher hydrophobic character compared to the prismatic planes or defects, and thus, was hardly impact the overall desulfurization activity. The decrease of the SSA could be directly attributed to the presence of the low SSA solid sulfur. Similar results have also been reported for the low-temperature desulfurization process on CNTs with dual hydrophilic/hydrophobic character [66]. Such residual solid sulfur deposited can be efficiently removed by a thermal treatment under helium at 320 °C according to the data collected. XPS analysis seems to indicate that during the regeneration process some sulfur may

be incorporated in the CNTs matrix or migrate deeper inside the channel and thus, remain presence after the treatment process. XPS analysis also indicates that part of the oxygen incorporated into the acid treated CNTs was removed during the course of the reaction and also during the regeneration process (Table 2). According to the catalytic results the oxygen lost seems to hardly influence the overall desulfurization activity. The O1s XPS results recorded on the fresh and spent O-CNT catalyst are presented in Fig. 11 and indicate that most of the oxygen lost was originated from the C—OH and C— O—C groups, i.e., 3.6 versus 2.5, while the C═O concentration remains almost unchanged before and after reaction, i.e., 2.9 versus 2.7. Taken into account that only carbonyl group is active for the reaction one can stated that the lost of the other oxygen species will not play a key role in the maintain of the desulfurization activity. The oxygen lost could be attributed to some side reactions between the oxygenated functional groups and the reactants during the course of the reaction. The advanced hypothesis was confirmed by the absence of any catalytic deactivation during the test despite such significant oxygen lost due to the low desulfurization activity of these oxygenated functional groups.

The results obtained in the present study have evidence one pivotal fact in the development of metal-free catalysts which is that catalytic process on carbon is strongly drive by carbon defects decorated with the oxygenated functional groups. According to the results the presence of hetero-atoms doping is not a *sine qua none* conditions in the synthesis of a highly active and stable metal-free catalyst and that the carbon surface containing oxygen decorated defects alone could also fulfill the request. The role of oxygen decorated defects acting as catalytic sites observed in this study is similar to that reported on metal-driven catalyst where the formation of carbon defects decorated with oxygen inside the parent metal oxide significantly improve the overall catalytic performance of the systems for performing dissociative adsorption of hydrogen and hydrocarbon in the selective isomerization process [67,68]. The main advantage of the O-CNT system in the present work is its extremely low sensitivity towards oxidation due to the lack of metal unlikely to that of the metal-oxygen-carbon defective systems which displaying an extremely high reactivity towards over oxidation upon air exposure. The results obtained also evidences the synergistic role of the nitrogen doping and defect sites on the desulfurization performance. It is expected that a combination of nitrogen doping and oxygen decorated defect sites could represent an interesting option for the development of a new generation of metal-free catalysts with improved catalytic performance not only for the selective oxidation process but also in other catalytic applications such as dehydrogenation or in electrochemistry energy storage.

The detailed investigation of the desulfurization performance has also pointed out the relatively high re-adsorption rate of the formed sulfur on the defect sites which favors the complete oxidation process leading to the formation of SO_2. Detailed investigation of the defect nature and sulfur re-adsorption rate as a function of the different reaction parameters will be conducted regarding the improvement of the sulfur selectivity on these catalysts.

4. Conclusion

In summary, we have shown that oxidation with gaseous HNO_3 can be an efficient and elegant pre-activation step to generate active metal-free catalysts, either without or with heteroatoms doping for performing partial oxidation process. According to the obtained results the nanodefects created on the CNT wall and the formation of oxygenated functional groups during the gaseous acid treatment could directly act as active phase for metal-free selective oxidation processes through dissociative adsorption of oxygen. This activation method is simple and allow one to avoid post-activation treatment process such as filtration and washing steps and shows better efficiency for the direct synthesis of metal-free carbon-based catalysts. The as-treated metal-free catalyst displays a high desulfurization performance along with an extremely high resistance towards deactivation as a function of time on stream, even at high space velocity or low O_2-to-H_2S ratio, which could be attributed to the high stability of the oxygen decorated defects playing the role of active sites. The high stability of the O-CNT catalyst after reaction at low O_2-to-H_2S ratio is of extreme interest. Indeed, for the state-of-the-art iron oxide catalyst a deficient in oxygen supply leads to an irreversible deactivation of the catalyst due to the problem of surface sulfidation. The sulfur selectivity on the O-CNTs catalyst is somewhat lower compared to that obtained on the iron oxide catalyst and could be attributed to the presence of strong adsorption sites, i.e., adjacent defects, which favor the complete oxidation of the formed sulfur into SO_2. It is expected that the results obtained here will contribute to the future development of metal-free carbon-based catalysts with better catalytic performance and stability compared to the traditional metal and oxides supported ones in numerous catalytic processes. Additional work will be carried on these nanocarbon materials with macroscopic shaping for further industrial development. Finally, the gas-phase acid treatment described in this work will be extended to other forms of carbon, such as few-layer graphene, expanded graphite and microfilamentous carbon, with the aim to developing new class of metal-free catalysts with low environmental impact.

Acknowledgements

The present work is conducted within the framework of the 7th European program (FREECATS) under a contract number of NMP3-SL-2012-280658. DVC would like to thank the Vietnamese government for the grant during his stay at the ICPEES. The SEM and TEM analysis were performed at the facilities of the IPCMS (UMR 7504) and W. H. Doh and T. Romero (ICPEES) are gratefully acknowledged for performing XPS and SEM analysis. Prof. O. Ersen (IPCMS) is gratefully acknowledged for helpful discussion of the TEM results.

References

[1] D.S. Su, S. Perathoner, G. Centi, Chem. Rev. 113 (2013) 5782–5816.
[2] P. Serp, M. Corrias, P. Kalck, Appl. Catal. Gen. 253 (2003) 337–358.
[3] J.-P. Tessonnier, D.S. Su, ChemSusChem 4 (2011) 824–847.
[4] C. Pham-Huu, M.-J. Ledoux, Top. Catal. 40 (2006) 49–63.
[5] J. Amadou, K. Chizari, M. Houllé, I. Janowska, O. Ersen, D. Bégin, C. Pham-Huu, Catal. Today 138 (2008) 62–68.
[6] M.J. Ledoux, R. Vieira, C. Pham-Huu, N. Keller, J.Catal. 216 (2003) 333–342.
[7] J. Zhang, X. Liu, R. Blume, A. Zhang, R. Schlögl, D.S. Su, Science 322 (2008) 73–77.
[8] J.-M. Nhut, R. Vieira, L. Pesant, J.-P. Tessonnier, N. Keller, G. Ehret, C. Pham-Huu, M.J. Ledoux, Catal. Today 76 (2002) 11–32.
[9] J. Zhang, D. Su, A. Zhang, D. Wang, R. Schlögl, C. Hébert, Angew. Chem. Int. Ed. 46 (2007) 7319–7323.
[10] Y. Peng, H. Liu, Ind. Eng. Chem. Res. 45 (2006) 6483–6488.
[11] J.M. Simmons, B.M. Nichols, S.E. Baker, M.S. Marcus, O.M. Castellini, C.-S. Lee, R.J. Hamers, M.A. Eriksson, J. Phys. Chem. B 110 (2006) 7113–7118.
[12] H. Hiura, T.W. Ebbesen, K. Tanigaki, Adv. Mater. 7 (1995) 275–276.
[13] K.J. Ziegler, Z. Gu, J. Shaver, Z. Chen, E.L. Flor, D.J. Schmidt, C. Chan, R.H. Hauge, R.E. Smalley, Nanotechnology 16 (2005) S539.
[14] I. Gerber, M. Oubenali, R. Bacsa, J. Durand, A. Gonçalves, M.F.R. Pereira, F. Jolibois, L. Perrin, R. Poteau, P. Serp, Chem. Eur. J. 17 (2011) 11467–11477.
[15] K.A. Wepasnick, B.A. Smith, K.E. Schrote, H.K. Wilson, S.R. Diegelmann, D.H. Fairbrother, Carbon 49 (2011) 24–36.
[16] S. Osswald, M. Havel, Y. Gogotsi, J. Raman Spectrosc. 38 (2007) 728–736.
[17] N.P. Blanchard, R.A. Hatton, S.R.P. Silva, Chem. Phys. Lett. 434 (2007) 92–95.
[18] B. Smith, K. Wepasnick, K.E. Schrote, H.-H. Cho, W.P. Ball, D.H. Fairbrother, Langmuir 25 (2009) 9767–9776.
[19] W. Xia, C. Jin, S. Kundu, M. Muhler, Carbon 47 (2009) 919–922.
[20] C. Li, A. Zhao, W. Xia, C. Liang, M. Muhler, J. Phys. Chem. C 116 (2012) 20930–20936.
[21] J. Zhang, D.S. Su, R. Blume, R. Schlögl, R. Wang, X. Yang, A. Gajović, Angew. Chem. Int. Ed. 49 (2010) 8640–8644.

[22] C. Duong-Viet, L. Truong-Phuoc, T. Tran-Thanh, J.-M. Nhut, L. Nguyen-Dinh, I. Janowska, D. Begin, C. Pham-Huu, Appl. Catal. Gen. 482 (2014) 397–406.
[23] C. Duong-Viet, H. Ba, Y. Liu, L. Truong-Phuoc, J.-M. Nhut, C. Pham-Huu, Chin. J. Catal. 35 (2014) 906–913.
[24] K. Chizari, A. Deneuve, O. Ersen, I. Florea, Y. Liu, D. Edouard, I. Janowska, D. Begin, C. Pham-Huu, ChemSusChem 5 (2012) 102–108.
[25] F. Sun, J. Liu, H. Chen, Z. Zhang, W. Qiao, D. Long, L. Ling, ACS Catal. 3 (2013) 862–870.
[26] Y. Liu, C. Duong-Viet, A. Hébraud, G. Schlatter, J. Luo, O. Ersen, J.M. Nhut, C. Pham-Huu, ChemCatChem 7 (2015) 2957–2964.
[27] X. Zhang, Y. Tang, S. Qu, J. Da, Z. Hao, ACS Catal. 5 (2015) 1053–1067.
[28] K. Gong, F. Du, Z. Xia, M. Durstock, L. Dai, Science 323 (2009) 760–764.
[29] L. Truong-Phuoc, C. Duong-Viet, W.-H. Doh, A. Bonnefont, I. Janowska, D. Begin, E.R. Savinova, P. Granger, C. Pham-Huu, Catal. Today 249 (2016) 236–243.
[30] G. Tuci, C. Zafferoni, A. Rossin, A. Milella, L. Luconi, M. Innocenti, L. Truong Phuoc, C. Duong-Viet, C. Pham-Huu, G. Giambastiani, Chem. Mater. 26 (2014) 3460–3470.
[31] X. Li, X. Pan, L. Yu, P. Ren, X. Wu, L. Sun, F. Jiao, X. Bao, Nat. Commun. 5 (2014).
[32] B. Zhong, J. Zhang, B. Li, B. Zhang, C. Dai, X. Sun, R. Wang, D.S. Su, Phys. Chem. Chem. Phys. 16 (2014) 4488–4491.
[33] D. Yu, E. Nagelli, F. Du, L. Dai, J. Phys. Chem. Lett. 1 (2010) 2165–2173.
[34] C. Shan, W. Zhao, X.L. Lu, D.J. O'Brien, Y. Li, Z. Cao, A.L. Elias, R. Cruz-Silva, M. Terrones, B. Wei, J. Suhr, Nano Lett. 13 (2013) 5514–5520.
[35] Y. Xue, B. Wu, L. Jiang, Y. Guo, L. Huang, J. Chen, J. Tan, D. Geng, B. Luo, W. Hu, G. Yu, Y. Liu, J. Am. Chem. Soc. 134 (2012) 11060–11063.
[36] Y. Xia, G.S. Walker, D.M. Grant, R. Mokaya, J. Am. Chem. Soc. 131 (2009) 16493–16499.
[37] L. Qu, Y. Liu, J.-B. Baek, L. Dai, ACS Nano 4 (2010) 1321–1326.
[38] S. Song, H. Yang, R. Rao, H. Liu, A. Zhang, Catal. Commun. 11 (2010) 783–787.
[39] K. Waki, R.A. Wong, H.S. Oktaviano, T. Fujio, T. Nagai, K. Kimoto, K. Yamada, Energy Environ. Sci. 7 (2014) 1950–1958.
[40] B. Frank, R. Blume, A. Rinaldi, A. Trunschke, R. Schlögl, Angew. Chem. Int. Ed. 50 (2011) 10226–10230.
[41] S. Wu, G. Wen, J. Wang, J. Rong, B. Zong, R. Schlögl, D.S. Su, Catal. Sci. Technol. 4 (2014) 4183–4187.
[42] S. Wu, G. Wen, R. Schlögl, D.S. Su, Phys. Chem. Chem. Phys. 17 (2014) 1567–1571.
[43] C.H. Collett, J. McGregor, Catal. Sci. Technol. (2015), http://dx.doi.org/10.1039/c5cy01236h.
[44] L. Connock, Sulphur 34 (1998) 257.
[45] S.W. Chun, J.Y. Jang, D.W. Park, H.C. Woo, J.S. Chung, Appl. Catal. B: Environ. 16 (1998) 235.
[46] J.W. Estep, G.T. McBride Jr., J.R. West, Advances in Petroleum Chemistry and Refining, vol. 6, Interscience, New-York, 1962, pp. 315.
[47] J. Wieckowska, Catal. Today 24 (1995) 405.
[48] M.J. Ledoux, C. Pham-Huu, N. Keller, J.B. Nougayrède, S. Savin-Poncet, J. Bousquet, Catal. Today 61 (2000) 157–163.
[49] J.H. Uhm, M.Y. Shin, J. Zhidong, J.S. Chung, Appl. Catal. B: Environ. 22 (1999) 293.
[50] E. Laperdrix, G. Costentin, N. Nguyen, F. Studer, J.C. Lavalley, Catal. Today 61 (2000) 149.
[51] D.D.E. Koyuncu, S. Yasyerli, Ind. Eng. Chem. Res. 48 (2009) 5223.
[52] R.J.A.M. Terörde, P.J. van den Brink, L.M. Visser, A.J. van Dillen, J.W. Geus, Catal. Today 17 (1993) 217.
[53] P. Nguyen, J.M. Nhut, D. Edouard, C. Pham, M.J. Ledoux, C. Pham-Huu, Catal. Today 141 (2009) 397.
[54] N. Keller, C. Pham-Huu, M.J. Ledoux, Appl. Catal. A: Gen. 217 (2001) 205.
[55] P. Nguyen, D. Edouard, J.M. Nhut, M.J. Ledoux, C. Pham-Huu, Appl. Catal. B: Environ. 76 (2007) 300–310.
[56] K. Chizari, I. Janowska, M. Houllé, I. Florea, O. Ersen, T. Romero, P. Bernhardt, M.J. Ledoux, C. Pham-Huu, Appl. Catal. Gen. 380 (2010) 72–80.
[57] G. Gulino, R. Vieira, J. Amadou, P. Nguyen, M.J. Ledoux, S. Galvagno, G. Centi, C. Pham-Huu, Appl. Catal. Gen. 279 (2005) 89–97.
[58] L.G. Cançado, A. Jorio, E.H.M. Ferreira, F. Stavale, C.A. Achete, R.B. Capaz, M.V.O. Moutinho, A. Lombardo, T.S. Kulmala, A.C. Ferrari, Nano Lett. 11 (2011) 3190–3196.
[59] B. Louis, G. Gulino, R. Vieira, J. Amadou, T. Dintzer, S. Galvagno, G. Centi, M.J. Ledoux, C. Pham-Huu, Catal. Today 102–103 (2005) 23–28.
[60] W. Zhou, S. Sasaki, A. Kawasaki, Carbon 78 (2014) 121–129.
[61] Á. Reyes-Carmona, M.D. Soriano, J.M. López Nieto, D.J. Jones, J. Jiménez-Jiménez, A. Jiménez-López, E. Rodríguez-Castellón, Catal. Today 210 (2013) 117–123.
[62] X. Zhang, G. Dou, Z. Wang, L. Li, Y. Wang, H. Wang, Z. Hao, J. Hazard. Mater. 260 (2013) 104–111.
[63] H.J. Freund, N. Nilius, T. Risse, S. Schauermann, Phys. Chem. Chem. Phys. 16 (2014) 8148–8167.
[64] K. Amakawa, L.L. Sun, C.S. Guo, M. Hävecker, P. Kube, I.E. Wachs, S. Lwin, A.I. Frenkel, A. Patlolla, K. Hermann, R. Schlögl, A. Trunschke, Angew. Chem. Int. Ed. 52 (2013) 13553–13557.
[66] N. Keller, C. Pham-Huu, M.J. Ledoux, Appl. Catal. Gen. 217 (2001) 205–217.
[67] P. Delporte, C. Pham-Huu, M.J. Ledoux, Appl. Catal. Gen. 149 (1997) 151–180.
[68] C. Pham-Huu, P. Del Gallo, E. Peschiera, M.J. Ledoux, Appl. Catal. Gen. 132 (1995) 77–96.